

Analysis of the Impacts of Wind on Final Approach Overshoot Using Historical Flight and Weather Data

Seong-min Han,^{*} Bae-seon Park,[†] and Hak-Tae Lee [‡]
Inha University, Incheon, Republic of Korea, 21999

Flights typically intercept the final approach path approximately ten to fifteen nautical miles from the runway threshold. In some cases, the flight will overshoot the path during the interception, which is called a final approach overshoot (FAO). FAO itself is not considered a serious safety issue; however, it can cause glideslope or localizer deviations that can subsequently lead to more serious safety issues such as a go-around or hard landing. Various factors can cause FAO, including weather, air traffic control instructions, pilot competence, or aircraft performance. In this paper, the effect of wind on FAO at four major airports in the Republic of Korea is analyzed using flight trajectory data and weather data in 2019. Wind components are interpolated from the weather data corresponding to the time and location of the final approach path interception points. The general distribution of wind speeds and directions is analyzed by plotting wind roses. A positive correlation between the probability of FAO and the magnitude of the crosswind is observed for most airports and runways, while each airport has its own characteristics. Using the methods presented in this paper, the impact of wind at each airport can be identified with quantitative probability, and it can be used to establish specific guidelines for air traffic control and pilots to reduce FAO.

I. Introduction

STATISTICS from the International Air Transport Association show that over the past five years, the landing phase of flight has seen the highest number of accidents [1]. During the approach phase of a landing, an aircraft aligns its course with the runway. A large deviation from the extended centerline of the runway while intercepting this line is called Final Approach Overshoot (FAO). FAO can result in an unstable approach in terms of glideslope deviation (GS) or localizer deviation (LOC), which can lead to more serious safety problems such as go-around or hard landing. Park *et al.* [2] analyzed the approaching flights on Runway 25 of Jeju International Airport (CJU) and constructed a probability tree model for the subsequent events. When a flight experiences a long FAO, defined as an FAO lasting more than 30 seconds, the probability of subsequent GS is about 50%, which is significant. On the other hand, the probability of subsequent LOC is about 1%.

Various factors such as weather, air traffic control instructions, pilot competence, or the performance of the aircraft can affect FAO. Han *et al.* [3] analyzed the distribution of the speeds from the runway threshold, and found that the speeds of the flights with FAO were consistently higher than the normal flights, with the difference is the largest around the intercept point.

In this paper, the impacts of wind on FAO are analyzed at four major airports in the Republic of Korea, Incheon International Airport (ICN), Gimpo International Airport (GMP), Gimhae International Airport (PUS), and CJU, using the historical trajectory data and weather data in 2019. Automatic Dependent Surveillance - Broadcast (ADS-B) data purchased from FlightAware is used for the trajectory data. Korean Local Analysis and Prediction System (KLAPS) data is used for the weather data. The three-dimensional position and time of the aircraft at the maximum overshoot location is determined and the wind is inferred by interpolating the KLAPS data in position and time.

In the majority of the cases, the probability of FAO shows a strong positive correlation with the crosswind. However, when the headwind is strong, the probability of FAO decreases.

Following this introduction, Section II describes the FAO geometry and analysis methodologies. Section III describes the weather data and the pre-processing steps to extract relevant wind information. Section IV presents the analysis results with a discussion for each airport. Finally, Section V concludes the paper.

^{*}M.S. Studnet, Department of Aerospace Engineering, 36 Gaetbeol-Ro, Yeonsu-Gu, Incheon.

[†]Post Doctoral Fellow, Industrial Science Technology Research Institute, Inha University, Incheon.

[‡]Professor, Department of Aerospace Engineering, 36 Gaetbeol-Ro, Yeonsu-Gu, Incheon, AIAA Senior Member.

II. Final Approach Overshoot

Figure 1 shows a conceptual drawing of a final approach intercept with a large overshoot to illustrate the geometry. To be considered as an overshoot, the flight must cross the extended runway center line and then the 2-D distance between the flight and the center line must decrease as the flight approaches the runway so that a maximum value exists. This maximum distance is recorded as the overshoot distance, which is calculated using the method described in [4]. Overshoot distance greater than 100 m is defined as FAO in this study.

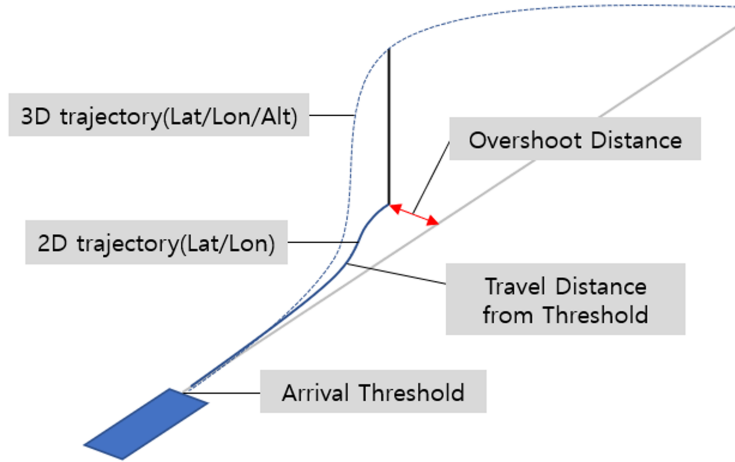


Fig. 1 Conceptual drawing of a final approach trajectory with an overshoot.

Figure 2(a) shows the trajectories of flights landing on Runway 36L at PUS. FAO can be seen within the area marked by the red oval. Figure 2(b) shows the distribution of the overshoot distance for the flights that landed on PUS Runway 36L. A total of 51,016 flights landed at this runway in 2019, and 3,378 flights are identified as FAO, meaning that the overshoot distance greater than 100 m.

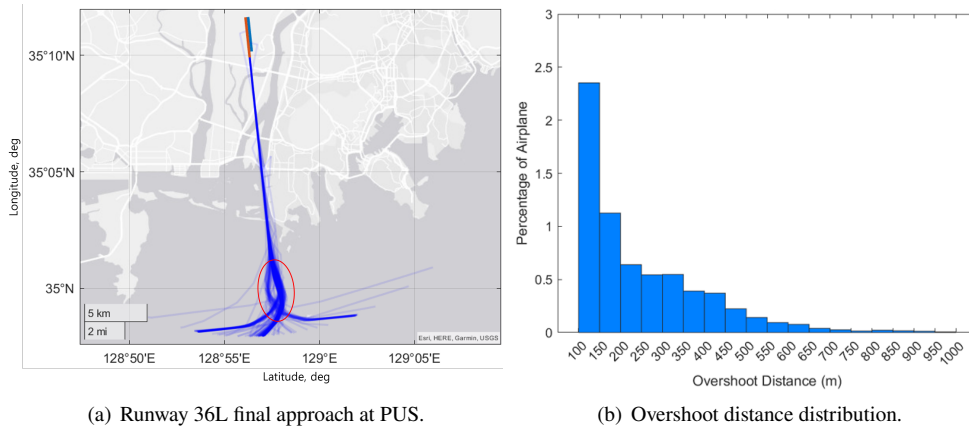


Fig. 2 Final approach path interception at PUS and the distribution of the overshoot distances.

The time interval of the ADS-B data used for this study is mostly in between five and ten seconds. The data, expressed in latitude and longitude, are projected onto a 2-D plane using the Lambert conformal conic projection, and then linearly interpolated to a regular one second interval.

III. KLAPS Weather Data

KLAPS weather data, provided by the Korea Meteorological Administration, is a large grid dataset represented by 235×283 horizontal grids spaced 5 km apart and 23 isobaric surfaces in the vertical direction [5]. The data are provided at one-hour intervals. At each grid point, the data include a variety of information, including air pressure, temperature, and geopotential height, in addition to the wind vectors. KLAPS also provides surface pressure and temperature.

A. Weather Data Pre-processing

Because the KLAPS data are not on a regular 3-D grid, using isobaric altitudes, the altitude of each grid point is slightly higher or lower as illustrated in Fig. 3. At each grid point, the vertical grid is interpolated at a regular 500 m intervals using the geopotential height information provided in the data.

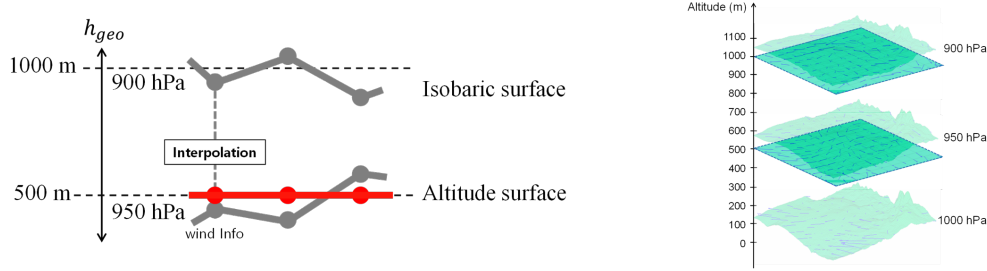


Fig. 3 Conversion process from isobaric to mean sea level.

B. Combining Trajectory Data and Weather Data

To combine trajectory data with weather data, a cube of eight grid points is identified in the KLAPS grid that contains the trajectory point at the given time. As the KLAPS data are given in one-hour intervals, the time interval must also be identified. The wind vector is found by a tri-linear interpolation using the cube of the nearest hour. The process is repeated for the cube of the next nearest hour and the two vectors are interpolated again using the time of the trajectory point as shown in Fig. 4.

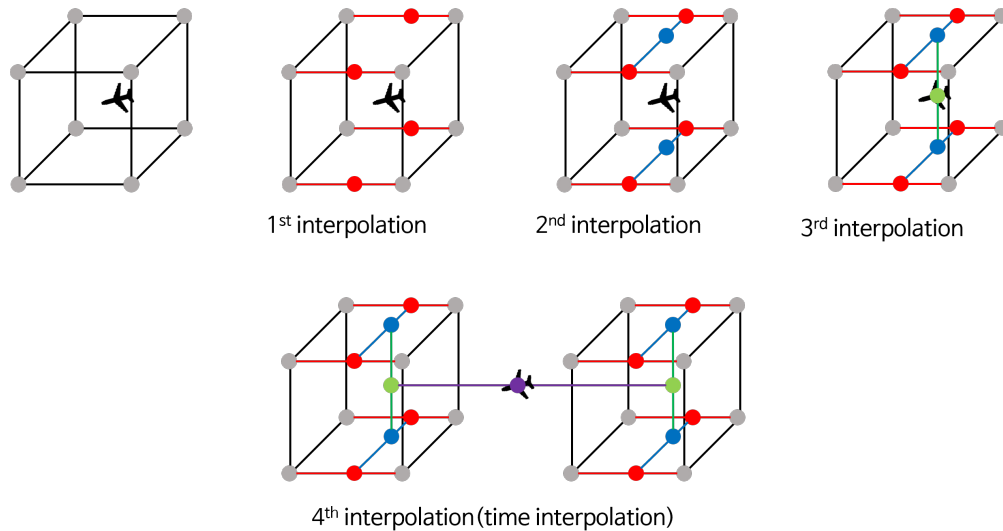


Fig. 4 Extracting the wind vector through interpolation.

C. Identifying Travel Distance for Extracting Wind

Figure 5 shows the two dimensional distribution of the overshoot distance as a function of the travel distance, which is the distance along track from the FAO point to the runway threshold. As can be seen from the red box shown in Fig. 5, the range of travel distances is identified where the FAO points are concentrated. 1 nmi is added to the maximum value of this range and set as the reference travel distance. This process is repeated for each runway at each airport. For each flight landing at the given runway of a given airport, the wind is extracted at a point where the remaining travel distance is the reference travel distance using the interpolation described in the previous subsection.

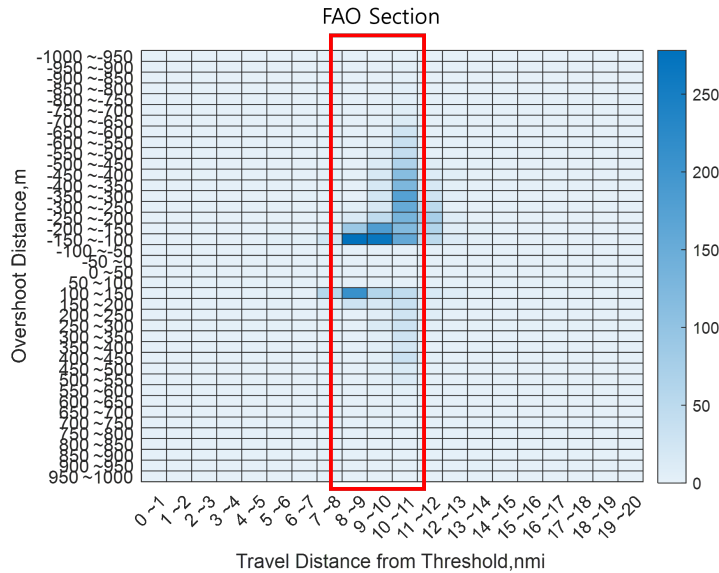


Fig. 5 Heat map of FAO points for PUS 36L approach.

IV. Analysis Results

Table. 1 summarizes the FAO results by airport and runway. The FAO probability ranges from 0.46% to 9.6%. Reference travel distances are also listed in Table. 1. As each runway has a different arrival procedure, it varies between nine and fourteen nmi.

Table 1 Summary of the FAO results.

Airport	PUS	GMP			ICN				CJU	
	Runway	36L	14R	32L	32R	15L	16	33R	34	07
Number of Landings	51,016	18,193	24,964	28,469	33,739	13,201	107,172	32,722	51,422	36,187
Number of FAO	3,378	1,751	114	158	1,603	554	904	736	3,905	1,551
Percentage (%)	6.6	9.6	0.46	0.55	4.8	4.2	0.84	2.3	7.6	4.3
Travel Distance (nmi)	12	9	12	13	9	10	13	14	10	12

To analyse the impacts of the wind, the wind vectors are visualised as a wind rose, which is explained below. The wind rose is essentially a histogram plotted in a circular way so that the wind direction can be intuitively compared to any reference such as runway directions.

- 1) The direction of the wind is outward from the center.
- 2) Speed range is distinguished by color from dark blue to yellow.
- 3) The radial length of each color band represents the frequency.

Figure. 6 shows the wind rose for aircraft landing on Runway 36L at PUS with the explanation of direction, speed, and frequency. The Direction of the Runway 36L is marked for comparison. Note that the correction for magnetic

heading is applied to compare the runway and wind direction. It can be observed that the wind direction is more or less evenly distributed.

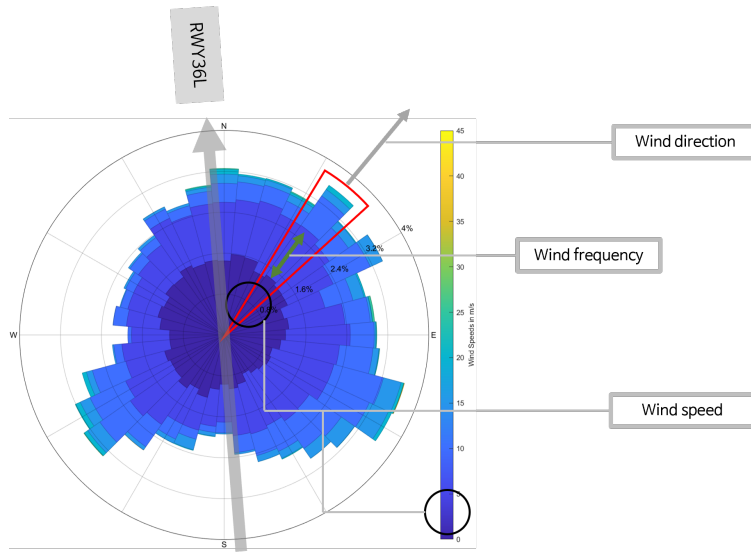


Fig. 6 Wind rose of PUS Runway 36L.

A. FAO and Wind Rose of PUS

The wind rose of Fig. 6 is further classified by FAO and non-FAO, called normal. FAO are further classified by positive which represents the interception while turning left and negative which represents the interception while turning right as shown in Fig. 7. Among the total 51,016 flights, 3378 flights are detected as FAO. 2,601 flights overshooted to the right side of the runway while making a left turn to intercept the final approach path. 777 flights overshooted to the left while making a right turn. The corresponding wind roses show the dominant directions of the crosswind, which are aligned with the direction of the overshoot.

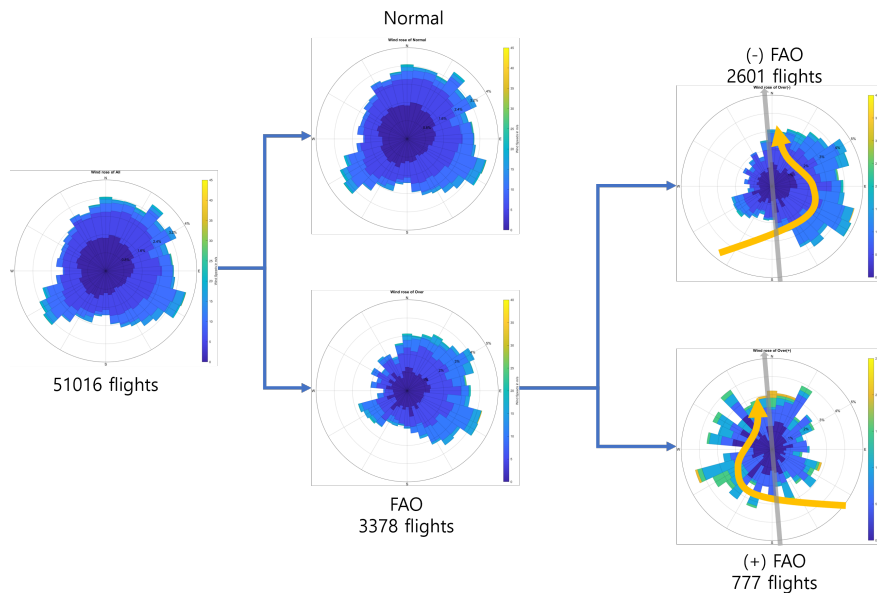


Fig. 7 Classification of the wind rose based on FAO and FAO directions.

Fig. 8 shows the percentage of FAO flights by the strength of the crosswind component. The crosswind component is the component of the wind that is perpendicular to the runway, and if the wind is headwind or tailwind, the crosswind component is zero. The FAO percentage is the percentage of FAO flights out of the total number of flights that land in the same crosswind range. Fig. 8 shows the probability distribution of FAO in positive and negative directions. For example, for the negative direction, the probability of FAO is around twelve% when the crosswind is between ten to fifteen m/s, which means among all the aircraft landed while experiencing the same amount of crosswind at approximately twelve nmi South of the runway threshold, twelve percent of the flight overshooted over 100 m from the extended runway center line. The positive correlation between the strength of the crosswind and the FAO probability is clearly visible in Fig. 8 for both the FAO directions.

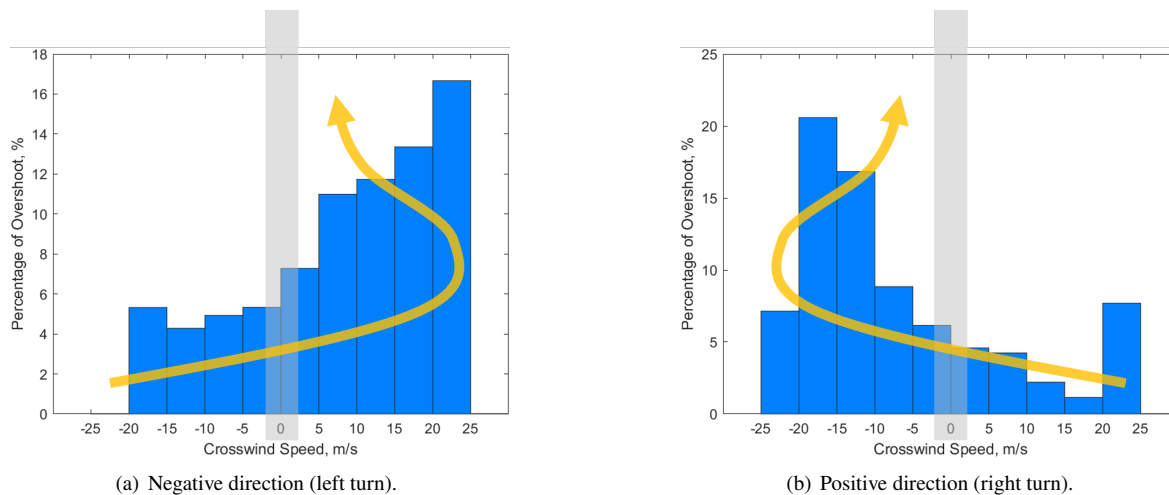


Fig. 8 FAO probabilities by crosswind strengths.

B. FAO and Wind Rose of GMP

Of the 18,193 flights that landed on Runway 14R at GMP in 2019, 1,751 flights had FAO. This is the highest percentage in Table 1. Fig. 9 shows the wind roses for the normal and FAO flights. The wind rose for the normal flights shows a strong crosswind bias in both directions, while the wind rose for the FAO flight is dominated by the crosswind components in the direction of the overshoot. In Fig. 10, the FAO probabilities for flights landing on Runway 14R are shown. Similar to the Runway 36L at PUS, the probability increases as the crosswind in the overshoot direction increases.

24,964 and 28,469 flights landed on Runways 32L and 32R, with 114 and 158 detected FAO, respectively. Figure 11 shows the wind rose for Runway 32L, which is dominated by headwinds. It can be observed that, for GMP, the North flow mostly experiences favorable headwind conditions while the South flow is dominated by unfavorable crosswind conditions. The difference in the wind pattern shows in the FAO percentage in Table 1 where the North and South flow shows 10% and 0.5% FAO, respectively. Figure 12 shows the FAO probability. Unlike the Runway 14R, it does not display a clear correlation, because the crosswind component as well as the number of sample is small. Almost identical trend is observed at Runway 33R.

C. FAO of ICN

As ICN is close to GMP geographically, 33 km apart, and the runway directions are within ten degrees, similar trends as GMP are observed. North flow, landings on Runways 33R and 34 are dominated by headwind with smaller FAO probabilities while the South flow, landings on Runway 15L and 16 experience more crosswinds. Figure 13 shows the FAO probabilities, which is similar to GMP Runway 14R shown in Fig. 10. In general, the FAO probabilities at ICN is smaller than GMP, which is likely due to the fact that most of the flights at ICN are international flights using larger aircraft.

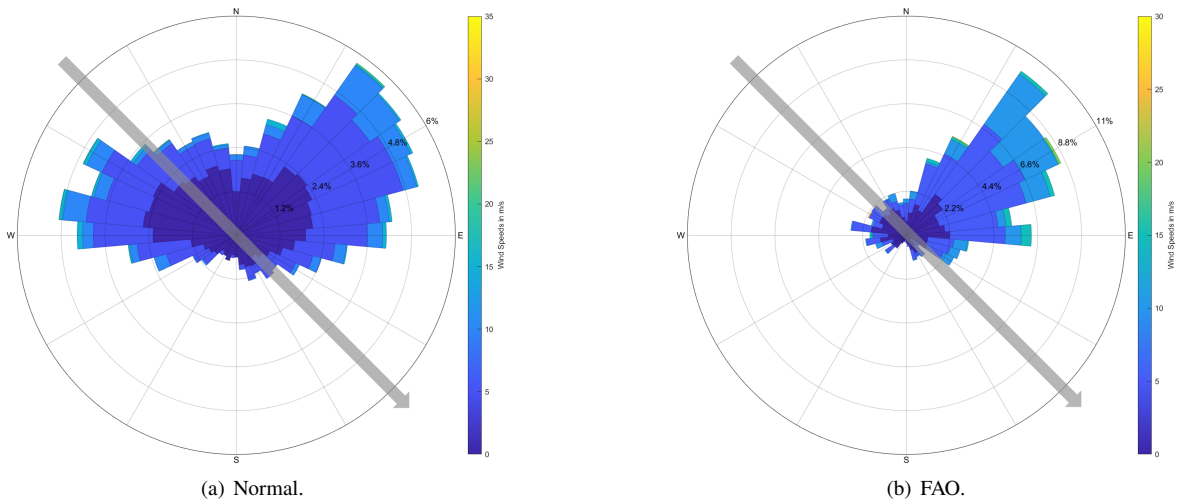


Fig. 9 Wind rose of GMP Runway 14R.

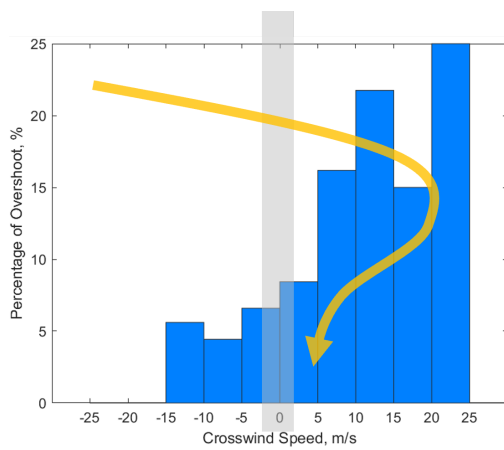


Fig. 10 FAO probability of GMP Runway 14R.

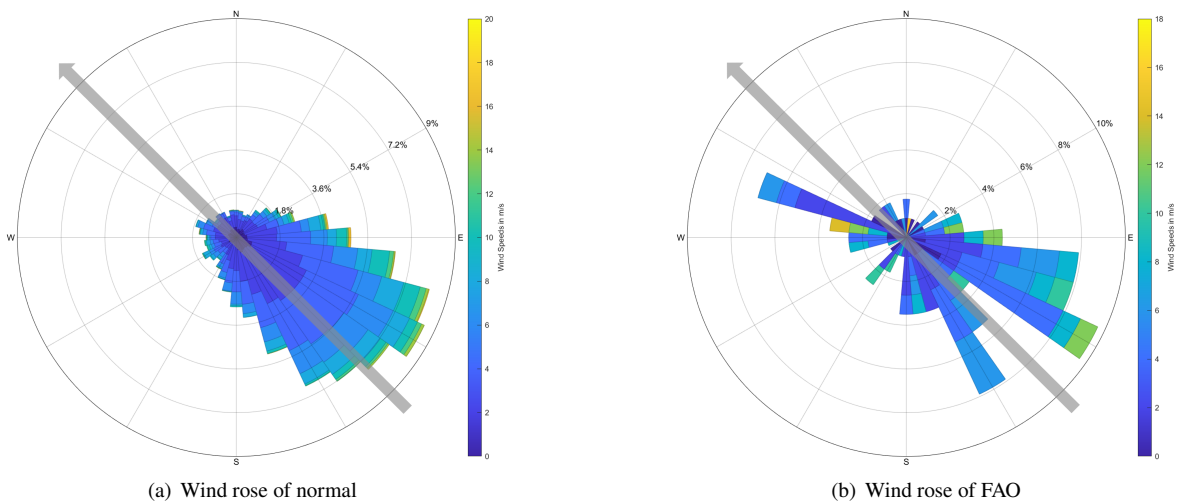


Fig. 11 Wind rose of GMP Runway 32L.

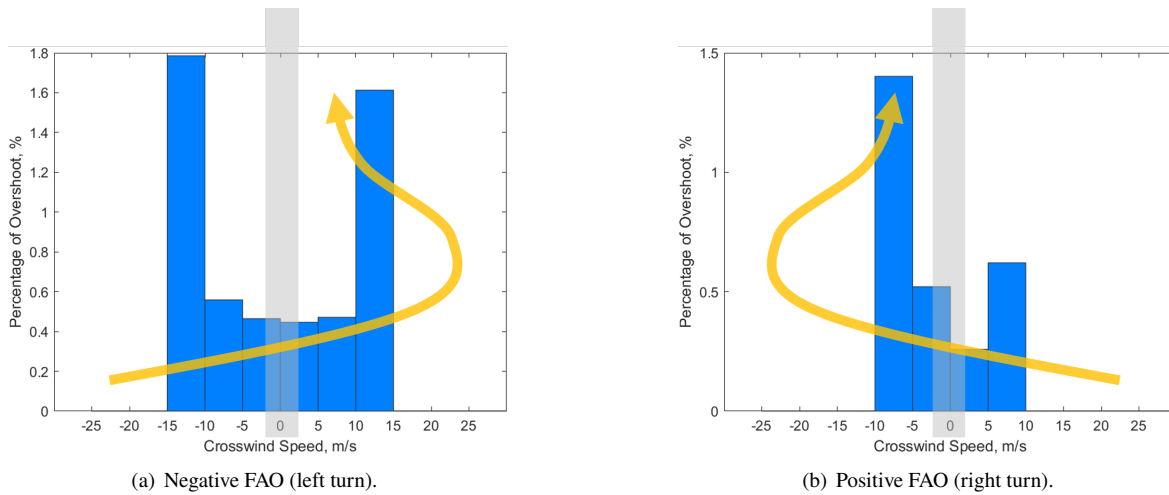


Fig. 12 FAO probability of GMP Runway 32L.

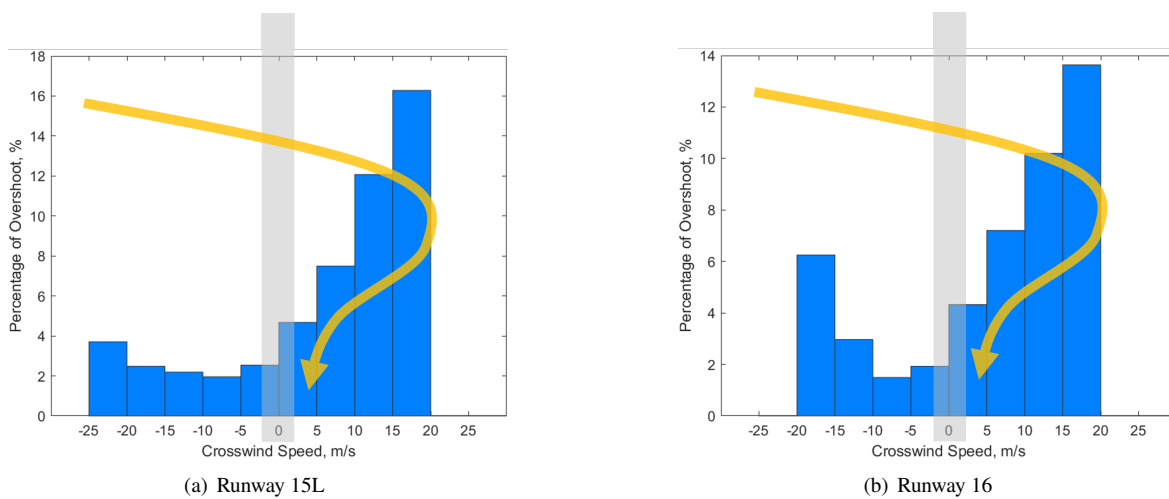


Fig. 13 FAO probabilities of ICN Runways 15L and 16.

D. FAO and Wind Rose of CJU

Most flights landing on CJU’s Runway 07 experience headwind as shown in Fig. 14. Even the flights with FAO are dominated by headwind as shown in Fig. 14(b). However, the total percentage of FAO is much larger than the North flow of ICN or GMP. In addition, the FAO probability distribution does not show clear correlation between the probability and the crosswind component.

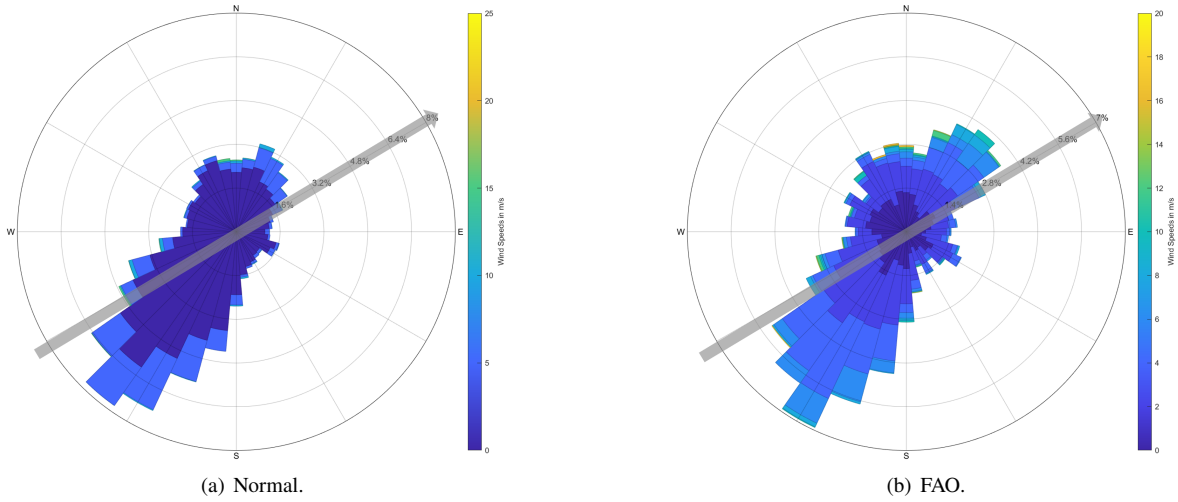


Fig. 14 Wind rose of CJU Runway 07.

Figure 15 shows the wind rose for CJU Runway 25, which is dominated by crosswind. However, the total FAO probability is actually smaller than the Runway 07 landings. The probability distribution of the positive FAO (right turn) shown in Fig. 16(b) shows positive correlation between the crosswind strength and the probability similar to the South flows of GMP and ICN. The FAO pattern at CJU need further investigation.

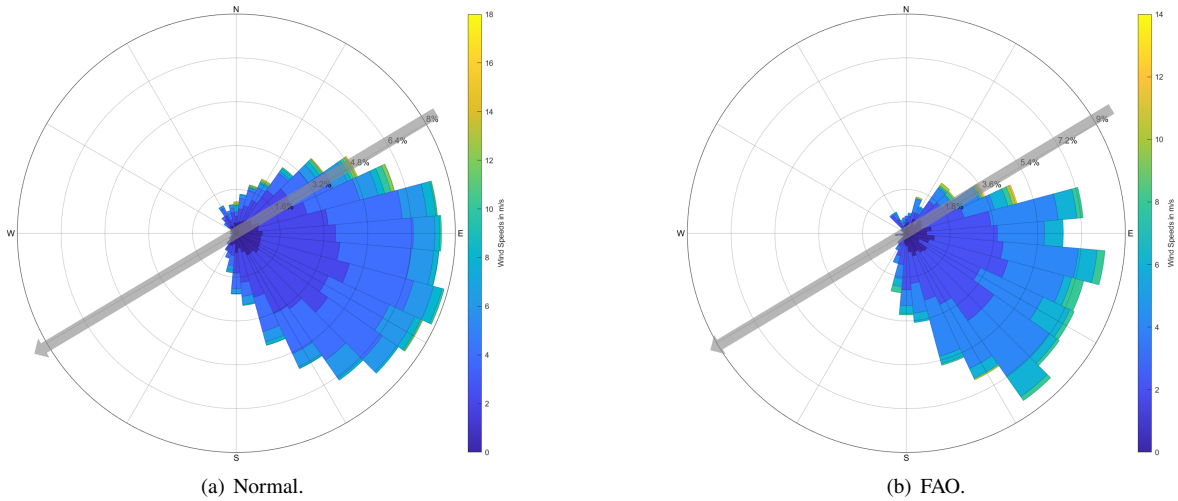


Fig. 15 Wind rose of CJU Runway 25.

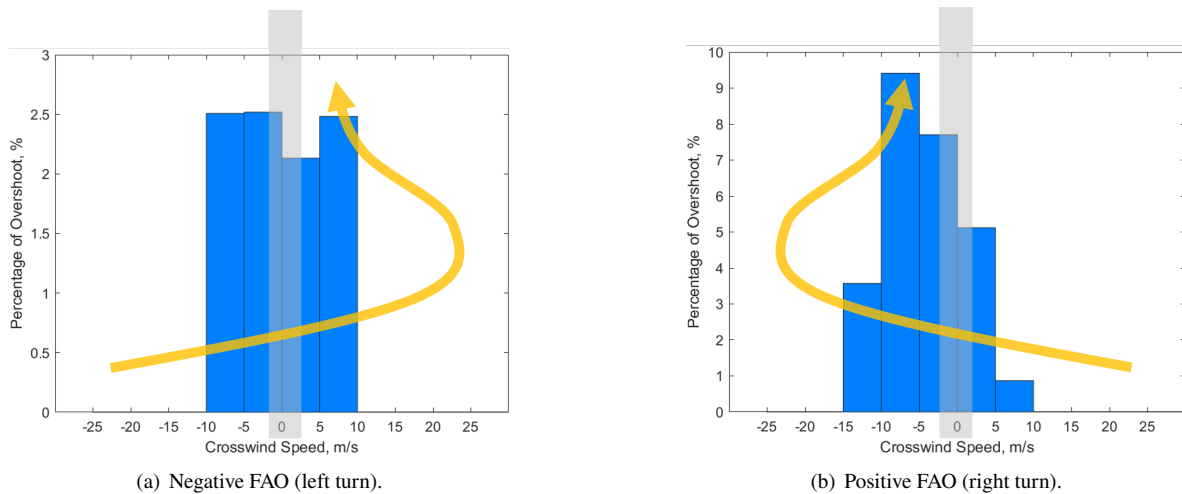


Fig. 16 FAO probability of CJU Runway 25.

V. Conclusions

In this paper, historical flight data and weather data are combined to analyze the correlation between wind and FAO. The analysis revealed that the percentage of FAO is very small for runways with well-aligned prevailing wind direction distribution. For the runways with relatively uniform wind direction distribution, FAO showed a strong correlation with the crosswind. In particular, the percentage of FAO flights for the same crosswind component showed a consistent trend. This analysis can be useful for predicting the FAO probability during actual operation based on the current wind condition. In addition, a simplified air traffic control strategy such as adjusting the interception initiation point or speed can be developed for each runway to reduce FAO.

Acknowledgments

This work was supported by Korea Agency for Infrastructure Technology Advancement (KAIA) grant funded by the Ministry of Land, Infrastructure and Transport (Grant RS-2020-KA158275) and by the National Research Foundation of Korea (NRF) (No. RS-2023-00258573) funded by the Ministry of Science and ICT.

References

- [1] IATA, “2021 Safety Report,” 2022.
- [2] Park, B.-S., Han, S.-M., Lee, H.-T., Lim, H., Byeon, H., and Jung, H.-J., “Detection and Analysis of Aviation Safety Events using Historic Flight Data,” *2023 IEEE/AIAA 42nd Digital Avionics Systems Conference (DASC)*, 2023, pp. 1–7. <https://doi.org/10.1109/DASC58513.2023.10311190>.
- [3] Han, S.-M., Park, B.-S., and Lee, H.-T., “2019 Gimhae International Airport Final Approach Overshoot Analysis,” *Proceeding of the 2023 KSAS Spring Conference*, 2023, pp. 1019–1020.
- [4] Han, S.-M., Park, B.-S., and Lee, H.-T., “Development of Final Approach Overshoot Calculation Algorithm,” *Proceeding of the 2022 KSAS Fall Conference*, 2022, pp. 1138–1139.
- [5] Kim, J., “ANNUAL REPORT 2017,” Korea Meteorological Administration 11-1360000-000999-01, 2017.